Segmentation of Forest Vegetation Layers Based on Geometric Features Extracted from 3D Point Clouds[1]

Segmentierung der Waldvegetationsschichten anhand von geometrischen Merkmalen aus 3D-Punktwolken

Mona Goebel, Jakob Schmidt und Dorota Iwaszczuk

The analysis of forest vegetation at lower heights, up to 2 m, is the focus of this work, while previous approaches primarily focused on trees and their stems. We calculated geometric metrics of point clouds, based on airborne, unmanned, and mobile laser scanning, to segment different vegetation growths and densities. Our results show that metrics based on eigenvalues such as planarity, linearity, and sphericity, as well as normal change rate are useful to differentiate forest layers in our scenario. Volume density is ineffective here as it is highly dependent on the data collection method. Roughness and principal component analysis in main direction (PCA1) do not show significant differences in vegetation growth and height. This research lays the foundation for the usage of geometric metrics to highlight growth and density changes in 3D vegetation and to differentiate forests into different layers without extensive processing.

Keywords: *Metric, mobile laser scanning, airborne laser scanning, UAV laser scanning, forest, vegetation, segmentation*

Die Analyse der Waldvegetation in niedrigeren Höhen, bis zu 2 m, steht im Mittelpunkt dieser Arbeit, während bisherige Ansätze sich hauptsächlich auf Bäume und ihre Stämme fokussierten. Wir berechneten geometrische Metriken von Punktwolken, die auf luftgestütztem, Drohnen-gestütztem und mobilem Laserscanning basieren, um verschiedene Vegetationswuchshöhen und Vegetationsdichten zu segmentieren. Unsere Ergebnisse zeigen, dass Metriken auf der Grundlage von Eigenwerten wie Ebenheit, Linearität und Sphärizität sowie der normalen Änderungsrate sich in unserem Szenario als nützlich erwiesen, um Waldschichten zu unterscheiden. Volumendichte ist hier ineffektiv, da sie stark von der Methode der Datenerfassung abhängt. Die Rauheit und die Hauptkomponentenanalyse in Hauptrichtung (PCA1) zeigen keine nützlichen Unterschiede in Vegetationshöhe und -dichte. Diese Forschungsarbeit legt den Grundstein für die Verwendung geometrischer Metriken zur Hervorhebung von Wachstums- und Dichteveränderungen in der 3D-Vegetation und zur Unterteilung von Wäldern in verschiedene Schichten ohne umfangreiche Verarbeitung.

Schlüsselwörter: Metrik, mobiles Laserscanning, luftgestütztes Laserscanning, UAV-Laserscanning, Wald, Vegetation, Segmentierung

[1] Überarbeiteter und erweiterter Beitrag der 22. Internationalen Geodätischen Woche Obergurgl 2023

1 MOTIVATION AND THEMATIC CONTEXT

It is essential to have as much current knowledge of forest resources as possible, to keep track of their change over time, to understand these heterogeneous systems, and to best protect them.

Light Detection And Ranging (LiDAR) is a technique that can be utilised to generate a point cloud and the corresponding sensor is mounted on various platforms. This includes Airborne Laser Scanning (ALS), Terrestrial Laser Scanning (TLS), and Unmanned aerial vehicle Laser Scanning (ULS). ALS is mounted on airplanes, ULS on unmanned aerial vehicle (UAV), and TLS on tripods. Mobile laser scanning (MLS) is LiDAR mounted on mobile platforms carried by ground-based vehicles or humans. While TLS is moved between scans, MLS scans continuously during sensor movement. We refer to /Vosselman & Maas 2010/ for more information.

Laser scanning is a popular method for forest research, for example to investigate the regeneration of forests. /Heinzel & Ginzler 2019/ state that TLS allows a more accurate and complete coverage of trees, but an MLS is better for larger areas. For segmentation and classification of urban trees, /Weinmann et al. 2017/ use geometric features for binary point-wise supervised semantic classification, assigning labels to irregularly distributed 3D points, and focusing on tree points. Various methods have been developed segmenting trees from laser scanning data (/Burt et al. 2018/, /Bulatov et al. 2021/, /Krisanski et al. 2021/)

In contrast to many studies in which low forest vegetation is considered as noise, /Hamraz et al. 2017/ show how non-dominant trees can be segmented under the canopy by truncating the canopy using vertical point distribution in a grid. /Huo et al. 2022/ also show this using a voxel approach and symmetry features to detect individual trees and shrubs. To describe low forest vegetation, /Song et al. 2021/ use the Leaf Area Index (LAI) on ALS point clouds and a full waveform analysis. /Willim et al. 2019/ show that their method based on point distribution is suitable for detecting understory vegetation in a height between 0.8 m and 1.8 m in a beech forest.

This work evaluates geometric features for vegetation segmentation in a forest 3D point cloud, focusing on metrics that segment vegetation into different layers and densities, as well as distinguish vegetation from ground. These metrics are based on point distribution and are independent of sensor type, except for intensity. Intensity is the amount of light from the original laser beams which is reflected on objects and detected by the LiDAR sensor. We consider linear, curvature, surface, and volume density metrics, emphasizing the different facets of vegetation shapes. These metrics are tested on a point cloud collected with MLS, ULS and ALS in a park and forest environment.

Metric	Definition	Source
Roughness	local curvature behaviour of the curves and surfaces, or deviation from the plane	/Wilke 2002/
Volume density	*n* points per radius	
Normal change rate	angular change between normals	/Wilke 2002/
Planarity	$\frac{\lambda_2 - \lambda_3}{\lambda_1}$, with eigenvalues $\lambda_1, \lambda_2, \lambda_3$.	/Chehata et al. 2009/
Sphericity	$\frac{\lambda_3}{\lambda_1}$	/Chehata et al. 2009/
Linearity	$\frac{\lambda_1 - \lambda_2}{\lambda_1}$,	/Chehata et al. 2009/
Surface variation	$\frac{\lambda_3}{\lambda_1 + \lambda_2 + \lambda_3}$	/Chehata et al. 2009/
Principal component analysis in main direction (PCA1)	measure for the variance of a point cloud in main direction	/Russ et al. 2006/

Tab. 1 | Overview of tested metrics

2 METHOD

Our approach is based on the computation of common metrics on 3D laser point clouds. Our choice of metrics was influenced by the following work: /Wilke 2002/ explains the basics of geometric data processing, /Russ et al. 2006/ use PCA in their work, /Chehata et al. 2009/ conclude that metrics based on eigenvalues were the most relevant features after height and echo for their random forest, and lastly /Weinmann et al. 2017/ develope a simple to understand method based also on geometric features to segment vegetation. Our chosen metrics (*Tab. 1*) should describe the geometry of forest vegetation. Because vegetation includes both difficult shapes, such as tree crowns and shrubs, and simpler shapes, such as stems and the ground, we believe that a combination of metrics describing linear and curvature geometry is best.

The value for each point and metric is calculated based on the neighbouring points within a given radius *r*. The radius is selected based on the point density. Points with fewer than two neighbours are excluded from the result, because values cannot be calculated for this point. Thus, outliers are automatically omitted. Values cannot be calculated for many points if the radius is smaller than the average point distance in the point cloud because insufficient points fall within the radius. Additionally, important structures are lost. If the radius is several times greater than the average point distance, the point cloud's finer details, such as the distinction between path and grass areas, are reduced.

As few pre-processing steps as possible were done in this work because some vegetation can easily be mistaken for noise. Only distant outlier groups in the point clouds were removed manually.

For the segmentation, first the metrics were calculated and then the point cloud was divided into vertical and horizontal slices, with a slice width *w*. Thus, for example, each horizontal slice has the size

Xrange × *Yrange* × *w*. Here, the *Xrange* is defined from the point with the minimal *X* position to the point with the maximal *X* position in the corresponding slice. *Yrange* is defined accordingly.

The horizontal slices were grouped into (1) low vegetation, (2) medium vegetation and (3) high vegetation. The vertical slices were divided into the categories (1) meadow, none to minor vegetation, (2) medium vegetation, which has primarily shrubs, scattered trees, and little dense vegetation, and (3) dense vegetation, which has dense low forest vegetation. In all slices, the mean values were considered.

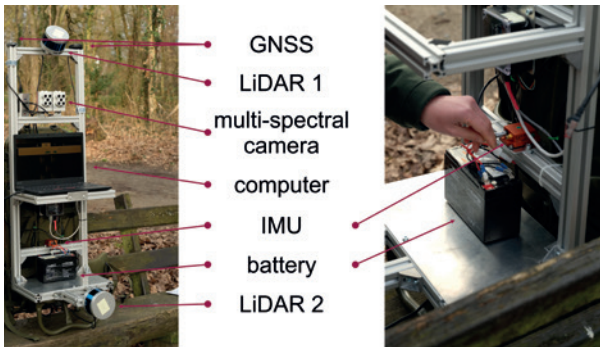

Fig. 1 | Components of the self-built multi-sensor backpack. The camera and lower LiDAR2 were not used in this work. /Photos: Lukas Einsele/

In addition, slices containing less than 1 000 points were excluded from the analyses.

The segmentation into the vegetation heights is based on thresholds that are taken from each dataset's metric graphs. As the used point clouds have no available reference data, the effectiveness of metrics' segmentation was evaluated visually, comparing the scene on-site and in the point cloud. A precise border between the vegetation groups is often not possible and are disputable. Therefore, a rough border in a range of half a meter was defined as sufficient. One example for such a border is between shrubs and taller trees, as the end of one and beginning of the next group is fuzzy.

To have a relative validation of the point cloud and real-world distances, human-built objects were measured on-site with a ruler, and digital in the point cloud using point to point distance measurements. Both cases included multiple measurements of the same distances and a calculated mean of these measurements.

3 EXPERIMENTS

For the investigations on MLS data, we collected point clouds with our self-built person-carried multi-sensor backpack. The backpack architecture is inspired by /Blaser et al. 2021/ and /Iwaszczuk et al. 2019/, hence ours also features an aluminium load carrier, an aluminium profile to mount the individual devices, two laser scanners

and an Inertial Navigation System (INS). The two laser scanners Velodyne VLP-16 Puck Lite have 16 rotating scan lines and were mounted in a similar way as /Blaser et al. 2021/ with the top at a 45° angle and the lower one at a 90° angle. At 1 m distance to the sensor the gap between the scan lines is approx. 86.2 mm, and the laser spots have a size of 15.4 mm × 11.0 mm. We included the Xsens MTi-700 INS, composing of an IMU and a GNSS antenna, to support the point cloud registration with movement information and global positioning. The orientation accuracy is 0.5° RMS in roll/pitch static and dynamic, and a 1.5° RMS in dynamic yaw. Including the GNSS antenna the positional error is 1 m horizontal and 2 m vertical, as stated by the manufacturer.

Other devices in the backpack include the laptop Lenovo ThinkPad 14s Gen 2, with a 52.5 Wh capacity battery, which powers the INS. The power source for the LiDARs is the LiFeEnergy 12V.19 LiFePO4 rechargeable battery. Additionally, the SLAM packages StaticMapping /Liu & atinfinity 2021/ and FastLIO /Xu & Zhang 2020/ were tested. StaticMapping considers the ordered accumulated Velodyne points as well as the angular velocity, the linear acceleration and GNSS positional information from the INS. In addition, the user sets the static transformations between the devices. The SLAM algorithm FastLIO does not take the GNSS information into account and estimates the static transformation of the devices automatically.

In this work, we only used the upper laser (LiDAR1), as we have found that the lower one does not add any benefit. The target-less extrinsic calibration between laser scanner and INS was performed using the open access code LI-Init by /Zhu et al. 2022/. Both devices were controlled via our ROS system, which is published here: https://git-ce.rwth-aachen.de/fg-fub/DeepForest/dp_ROS.git.

The ALS data was collected and provided by the Hessian Administration for Land Management and Geoinformation. The point cloud includes seven signal returns.

The ULS data was collected by Vermessung3D performed with a Matrice 300 RTK drone and a Zenmuse L1 sensor. Five flights were carried out over the same area, once in nadir and four times in 45° sensor angle from the four cardinal directions.

3.1 Study Areas

The study areas are all located in Darmstadt, Germany (*Fig. 2*). The study areas are subdivided into two experimental setups. The experimental setup A includes the types park (Park, *Fig. 2a*) and dense forest (Forest1, *Fig. 2b*), scanned by MLS on 15 and 24 September 2022. The setup B includes a forest path (Crossing, *Fig. 2c*) and a dense forest (Forest2, *Fig. 2d*), which were scanned by ALS, ULS and MLS. More precise, the forest path and dense forest were scanned by ALS in winter 2016 and ULS on 29 November 2022. The forest path was also scanned with MLS on 29 November 2022.

Experimental setup A in Park consists of a meadow with scattered trees, mostly in full leaf. The grass is brown and dry due to low summer rainfall.

The manual examination of the 3D point cloud was carried out in the area of the Park dataset. The objects included a path sign (6 distances measured) and a hydrant (1 distance measured). The measurements included a minimal distance of 30 cm and maximal 124 cm. The difference between in-situ and digital measurements is on average 0.98 cm and a standard deviation of 0.40 cm. As a result, the distances assumed in the point cloud relate to realistic distances. This result focused only on relative accuracy, not geo-referenced accuracy.

The Park dataset has a 56.9 m path and 13 million points, while Forest1's path is 73.3 m long and has 18 million points. A 63 m × 70 m *XY*-plane was cut from both datasets.

For MLS, no control points were available for the creation of the point clouds. Likewise, no GNSS could be used for registration in the forest because the dense canopy leads to erroneous GNSS data.

In the experimental setup B, the area Crossing covers approx. 14,855 m^2, ALS data containing around 340 thousand, ULS approx. 86 million and MLS approx. 69 million points. MLS data was primarily collected on forest paths due to dense vegetation, thus Crossing covering less area. Forest2 is a dense, unpaved forest with around 553 million points in ALS and 156 million in ULS data, covering 20,959 m^2.

3.2 Parameter Settings

The thresholds of the three height layers were chosen according to /Krieg 2020/, dividing horizontal slices into (1) low vegetation (≤ 0.5 m), (2) medium vegetation (0.5 – 2 m) and (3) high vegetation (≥ 2 m). Medium growth is crucial for hydraulic engineering and flood forecasting, which our research focused on.

After testing various radii, we chose 0.5 m radius for MLS and ULS metrics, while 1 m for ALS data due to its sparse point cloud. The radius remained constant across all metrics for better comparison. Horizontal and vertical slices were cut at width *w* of 0.5 m for all

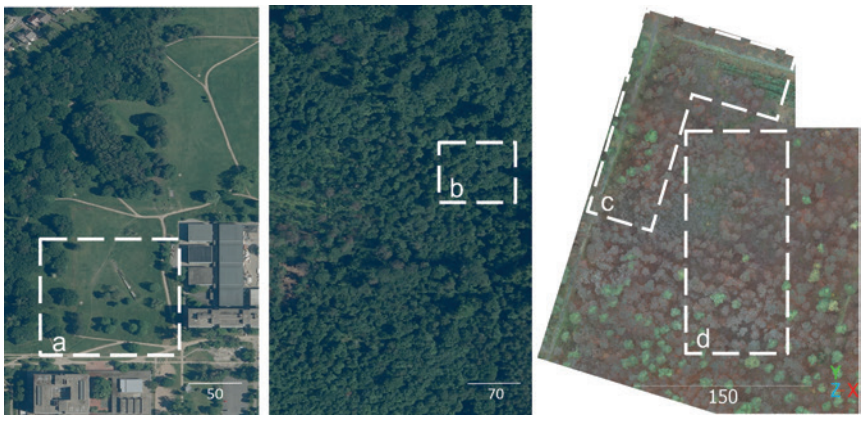

Fig. 2 | Overview of datasets, all located in Darmstadt, Germany. The dataset Park (a) and Forest1 (b) are shown over digital orthophotos from Hessian Administration for Land Management and Geoinformation from summer 2022. Crossing (c) and Forest2 (d) are visualised over the RGB coloured ULS data.

datasets. This width ensured a detailed analysis of the value changes regarding height and vegetation density. The width was not set lower, due to the amount of data this would produce.

The data processing was performed on a computer with an AMD Ryzen Threadripper 3960X 24-Core Processor, 256 GB RAM and a NVIDIA RTX A5000 GPU. The metric calculations and slicing were performed in the Software CloudCompare.

4 RESULTS AND EVALUATION

The SLAM algorithms StaticMapping and FastLIO were tested in post-processing. StaticMapping had visible difficulties in the Park (*Fig. 2a*) and especially in the Crossing dataset (*Fig. 2c*). In the latter case, it did not produce a reasonable point cloud. The poor quality was strongly visible based on the loop closure not successfully overlaying, leading to a large drift. In contrast, FastLIO could successfully close loops, but occasionally produced artefacts that resemble laser beams. These artefacts stood out because more points than usual occurred and were distributed in a linear line at a roughly 45° angle, which artificially increased the point density in this region. For example, in a region with a normal density of 1.9 points per 0.5 m radius, the density increases to a range of 157 to 895. Although we don't know why, we assume that the artefacts appear when the laser scanner is still for a few seconds. We could not successfully remove them, without altering the rest of the point cloud. Due to the indisputable better registration in the data Park, Crossing and Forest1, and similar results between the SLAM algorithms in Forest2, we have chosen the results of the FastLIO algorithm for all datasets, even though it included some noticeable artefacts.

A noise correction was unnecessary due to the exclusion of points with only one neighbour and omission of slices with less than 1 000 points.

In Section 4.1, we compare the metrics regarding vegetation height and vegetation density, only based on MLS data. In Section 4.2, we compare ALS, ULS and MLS point clouds, based on the conclusion from section 4.1.

4.1 METRIC COMPARISON

4.1.1 Comparison in Height

Roughness does not show a clear separation for different heights and objects (*Fig. 3*). In the low vegetation (0 – 0.5 m) the values of the *normal change rate*, *planarity*, *PCA1*, *surface variation*, and *roughness* are the same in Park and Forest1, respectively (*Tab. 2*). PCA1 shows no major changes in the point clouds.

Volume density is influenced by the scan location. The starting and end point (red area) and the walking path (green area) are visible in *Fig. 3*. In Forest1 the density is higher than in Park up to the height of 11.5 m. The volume density declines with increasing height, which derives from the increasing distance from the sensor and the decreasing vegetation (*Fig 3*, *Tab. 2*).

Planarity value behaviours for Park and Forest1 are similar. They both have a drop between 0.5 and 2 m (*Fig. 4*, *Tab. 2*). Visual distinction in the point clouds is represented by the ground (red) and a transition to the tree trunks (green).

Sphericity and *normal change rate* deliver similar results, as they are both a measure of curvature. A jump in the lower height range is visible in the sphericity in contrary direction to the planarity (*Fig. 4*). The tree crown's beginning in Park is symbolized by the slope in sphericity at about 4.5 m, and its thickest point is at the peak, which is about 5 m high. Visually recognisable in the point clouds is the ground (blue) and the transition to the tree trunks (*Fig. 4*, blue to green). In a height

	Park			Forest1		
Height up to	0.5 m	2.0 m	16.0 m	0.5 m	2.0 m	26.5 m
Number of points [mil.]	5.35	0.52	1.82	3.49	1.58	5.01
Intensity	25.02	15.16	18.32	30.67	24.65	14.11
Normal change rate	0.04	0.17	0.20	0.04	0.11	0.12
Roughness	0.04	0.09	0.08	0.04	0.07	0.06
Planarity	0.76	0.31	0.26	0.76	0.44	0.30
Linearity	0.17	0.33	0.39	0.18	0.34	0.48
Sphericity	0.08	0.36	0.43	0.07	0.22	0.22
PCA1	0.53	0.50	0.55	0.53	0.54	0.60
Volume density [k]	26.97	1.23	1.12	16.85	8.22	1.22

Tab. 2 | Horizontal comparison of metrics in height between Park and Forest1 dataset (mil. equivalent to millions, k to thousands)

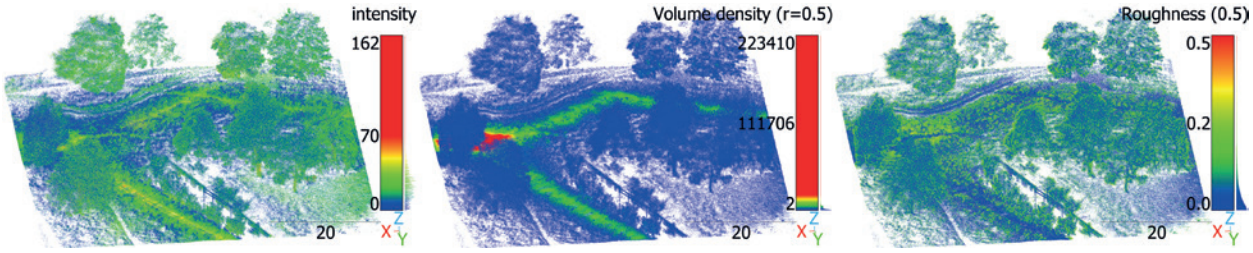

Fig. 3 | Metrics without meaningful distinctions, exemplary in the Park dataset. From left to right: intensity, volume density, roughness. A histogram showing the value distribution is located next to the legend. Red refers to high values, blue to low values. Volume density is number of points per sphere, others without unit.

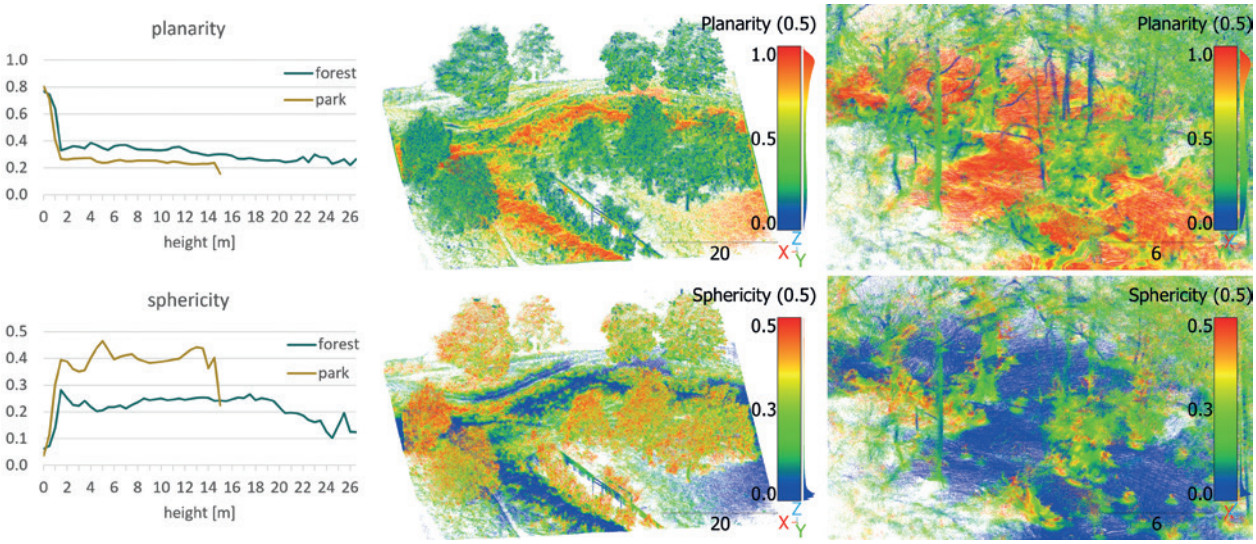

Fig. 4 | Planarity (top) and sphericity (bottom) in comparison. Park (middle) and Forest1 (right) coloured in the respective metric.

from 0.5 m to 2 m, sphericity is higher in Park (0.36) compared to Forest1 (0.22), likewise in the normal change rate. A possible reason for this could be the dominance of tree stems and human-made round objects such as a hydrant and a metal railing in the Park dataset.

Linearity increases with altitude noticeably (*Tab. 2*). One hypothesis for this is that lines appear more clearly in higher areas than in low or medium vegetation. However, it should also be noted here that FastLIO creates artefacts that influence the linearity. In the medium vegetation (0.5 – 2 m), the values are similar in both datasets.

Intensity is influenced by the walking path, as objects closer to the sensor tend to be measured with a higher intensity than objects further away (*Fig. 3*). Thus, the ground tends to have higher values. For a rough segmentation of tree stems and foliage the intensity is suitable, nevertheless. Tree stems and ground are stable and untransparent during the measurement, as well as reflect more light due to their larger surface. Thus, stems show a higher intensity than foliage.

The largest *number of points* is found in the low vegetation of Park (5.35 million, *Tab. 2*). The uneven ground in Forest1 decreases ground points in given height level. In both Park and Forest1, the number of points decreases in the medium vegetation. In Park, the tree stems are dominant in the medium height. The tree crowns are located above 2 m. The large trees in Forest1 provide a higher number of points (5.01 million) in the high growth than in Park (1.82 million). The maximum point cloud height is in Forest1 with 26.5 m, which is 10 m higher than in Park (*Tab. 2*).

4.1.2 Comparison in Density

For the investigation of different vegetation densities, the vertical slices are considered (*Tab. 3*). In Park these can be well divided into the areas meadow and medium-dense vegetation. Forest1 has dense vegetation throughout. It should be noted here that the number of points in the areas depends on the path, but can still reflect the three vegetation types well.

Vegetation density	Meadow	Medium-dense vegetation	Dense vegetation
Width *Y*	11 m	57 m	70 m
Number of points [mil.]	2.72	1.57	3.39
Normal change rate	0.04	0.14	0.11
Roughness	0.04	0.07	0.06
Planarity	0.77	0.42	0.39
Linearity	0.15	0.30	0.40
Sphericity	0.09	0.29	0.21
PCA1	0.52	0.51	0.57
Volume density [k]	20.07	87.94	286.77

Tab. 3 | Vertical comparison of metrics between Park (meadow and medium-dense vegetation) and Forest1 (dense vegetation)

In the dense vegetation, the *volume density* and *PCA1* values are higher than in the medium-density (*Tab. 3*). Increases between meadow and medium-dense vegetation can be seen in *sphericity*, *normal change rate* and *linearity*, as well as a decrease in *planarity* (*Tab. 3*).

In summary, metrics based on eigenvalues can be used reliably to distinguish vegetation heights and densities. Further, metrics that approximate geometric forms such as spheres, planes and lines, performed better than metrics highlighting point variance. In most cases, sphericity and planarity showed good results, as they emphasised round plants features and flat ground. In contrast, volume density and intensity are of limited use. They depend on the data collection approach and are influenced by sensor distance to objects. Regarding height, less points and a larger laser footprint were recorded in the MLS point clouds above 24 meters. Thus, it is challenging to generalize in higher slices.

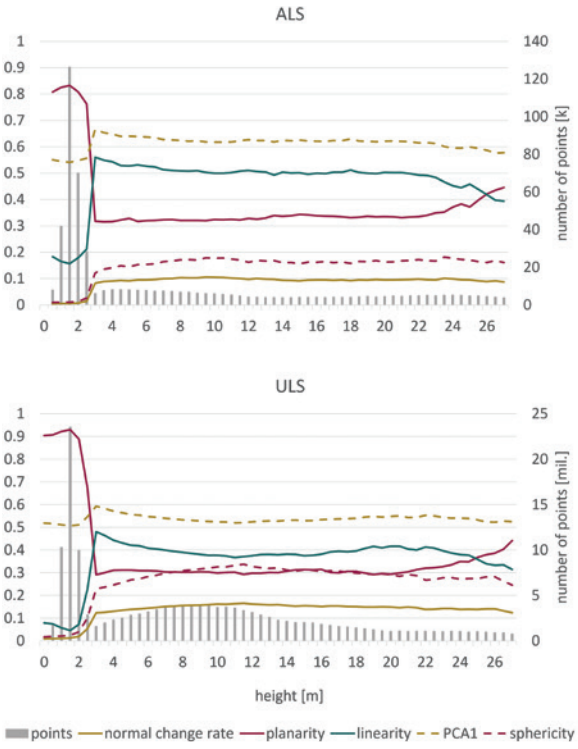

Fig. 5 | Average metric values per horizontal slice, calculated on Forest2

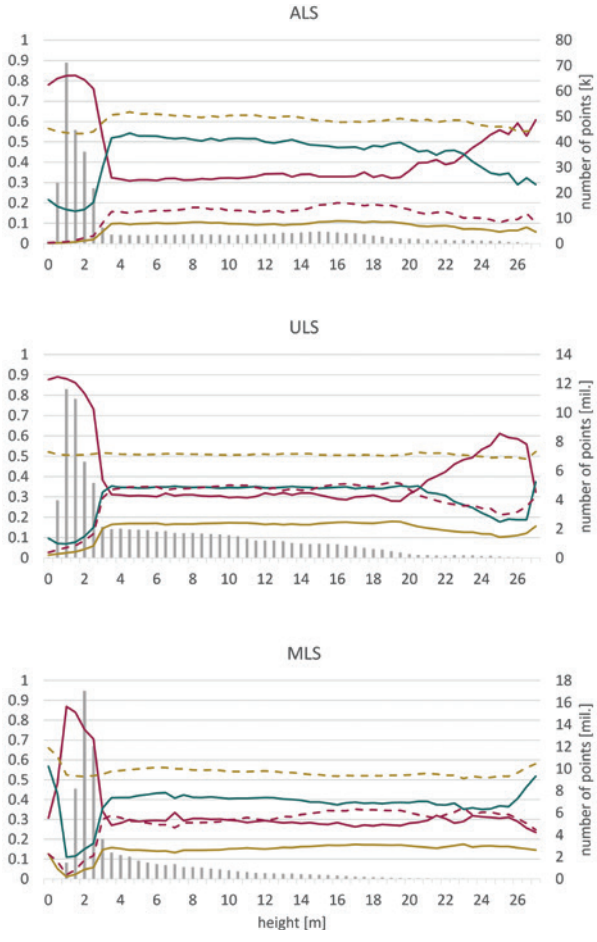

Fig. 6 | Average metric values per horizontal slice, calculated on Crossing

4.2 Comparison on Various Laser Scanning Types

Metrics were tested on other datasets to test if the useful metrics, namely normal change rate, planarity, linearity and sphericity, showed the same results on another type of laser scanning and in another area. Additionally, we focus on the value change in a height from zero to three meters. We added one meter, in order to reassure, if the border of 2 m is still the best fit.

Segmenting between vegetation heights is made based on the graphs in *Fig. 5* and *6*. However, this ought to extract the vegetation height threshold rather than metric values threshold. Dividing them only by metric value without slicing leads to points with the same value being scattered at various heights.

In a height of up to 3 m, the metric values change immense (*Fig. 5* and *6*). Another shift is visible at the tips of the tall tree crowns, approx. 24–26 m. For the dataset Crossing, the first slice has only 670 points in the ALS data and 23 points in the MLS data, which is why these slices are discarded. In the ULS data, however, it contains 53 228 points. Most points in all datasets are in the lower heights because of the large ground area. Noticeable however, is that in the ULS data relatively more points are in the heights 2 to 16 m, compared to ALS and MLS. The reason for less ALS points may be the occlusions caused by higher trees when scanning in nadir direction from above and for MLS an occlusion from below lower trees. An-

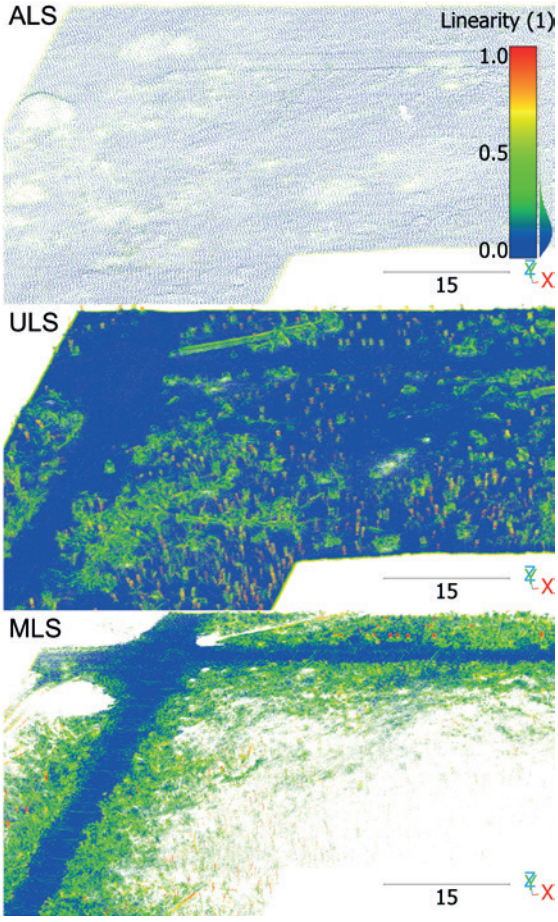

Fig. 7 | Crossing ALS, ULS and MLS point cloud coloured by linearity. Points above 3 m are excluded.

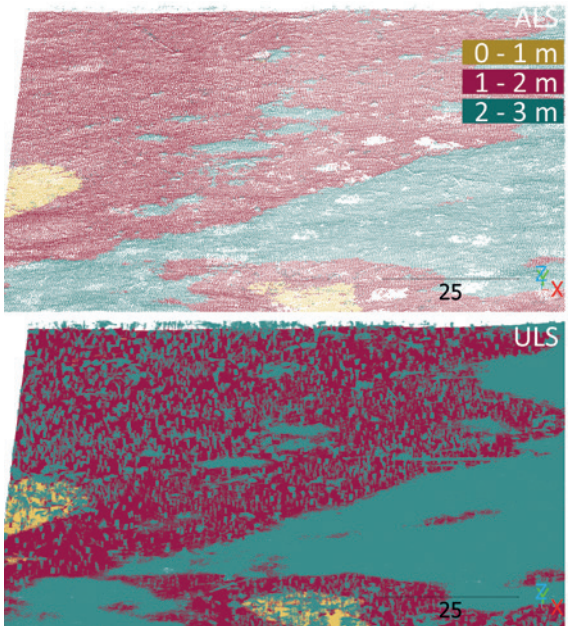

Fig. 8 | Forest2 ALS and ULS point cloud coloured by height. Points above 3 m are excluded.

other reason is that the ULS data is a summary of 5 flights in varying scan angles.

Both ALS and ULS show an even area of low linearity on the ground (blue) and small objects like deadwood and plants are well distinguishable (*Fig. 7*). MLS, on the contrary, strongly highlights the forest path in low linearity and the plants on the side in a higher value. Two main differences occur between MLS, ALS and ULS. MLS has a better view on the lower vegetation, but it is also affected by scanning angles. ALS and ULS always have the view from above the canopy, thus are less detailed in the vegetation beneath the canopy. Unlike MLS, they are not affected by the accessibility of the area. They all have less information on the lower vegetation in a dense forest, due to occlusions.

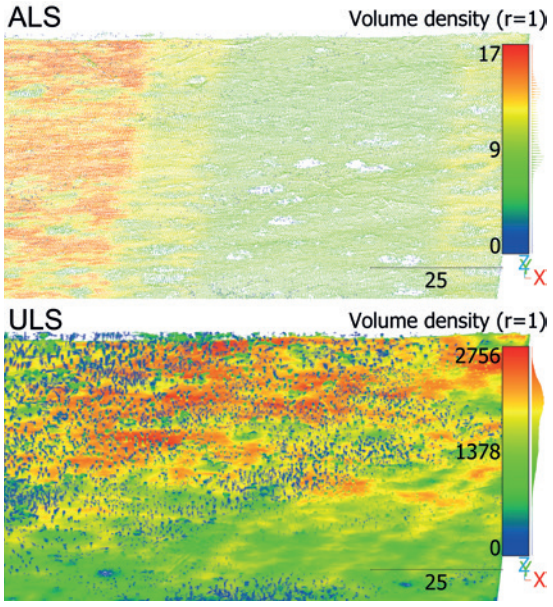

Fig. 9 | Forest2 ALS and ULS point cloud coloured by volume density. Points above 3 m are excluded.

Because the slices are cut based on the system's minimal point rather than the actual ground relief, the rough ground is visible at different heights (*Fig. 8*). Although the vegetation near the ground is important to examine, it is also the most prone to error. As a result, the metrics must be analysed with caution because they will differ depending on whether the area is ground or already vegetation.

Lastly, volume density is not only unreliable in MLS (*Fig. 3*), but also in ALS and ULS data (*Fig. 9*). In the ALS point cloud, the areas with overlapping flight strips have a higher number of points. Only in the ULS data, the data collection path is not noticeable, because the data consists of multiple paths from multiple flights. We can see that vegetation has a lower density (blue) than the ground. However, the density in this lower height is dependent on the amount of tree cover. The Forest2 area is densely vegetated by trees, resulting in fewer points reaching the forest floor, thus tendency to lower volume densities and a high diversity of volume densities depending on the overhanging vegetation.

5 DISCUSSION

Our results showed that planarity, linearity and sphericity were well suited to distinguish between forest levels. Further, normal change rate returned similar good results as sphericity. Volume density, intensity and roughness could not highlight significant changes in the vegetation.

When discussing point cloud heights, the importance of the system's origin or lowest point becomes apparent, since the height can be calculated using either the overall lowest point of the point cloud or the lowest point of the relevant pillar. The forest ground is not flat and can include slopes. While slicing the point cloud, one slice can include ground in one region and taller vegetation in the next region if the slope or unevenness is severe. In our case, we used the lowest point of the point cloud as height zero, as the areas are rather flat and even. Using a Digital Elevation Model (DEM) as a reference could be used in the pre-processing when there is a significant elevation change. These models, however, can miss fine elevations when scanning from above the canopy because they are based on ALS data. In general, we should state that ground and meadow below 0.5 meters should not be distinguished further, when using a slicing method. Our study showed that the metrics can be used for segmenting ground and vegetation, without using a slicing method. Such a generalisation is not possible for the segmentation of forest vegetation layers.

For the MLS and ULS point clouds, we chose a radius of 0.5 m, and for the ALS data a radius of 1 m. Our aim was to retain as much detail as we could without losing too many points or smoothing out the objects. When adapting this approach, the user is advised to recheck the best radius for their given data. Our approach has the advantage of not requiring a separate outlier removal because the metric calculations and slicing exclude them.

Using simple metrics results in a quick processing method. Note that the processing time is always proportional to the number of points. Unlike /Weinmann et al. 2017/ we did not downsample our data. We could process 5 metrics at a time in the ALS data in seconds, and the ULS data in 5 to 15 minutes. Therefore, we assume that our approach works on a wide range of computer configurations.

We did not use the extensive voxel approach in our analysis, because the precise shape of the vegetation is not the focus of this work. Our method is simple and quick slicing point clouds at a chosen threshold and width. If a fast and rough segmentation of the vegetation is desired, the slicing approach should be used. If precise segmentation is desired, the analysis should be followed by finer areal segmentation, or thinner slices.

Lastly, the presented metrics describe 3D vegetation distribution and rough geometry. This information can be converted into 2D images while preserving the 3D information. This extends the idea of only using height information of a point cloud, when fusing it with other data types.

6 CONCLUSION AND OUTLOOK

In this work, with geometric features we segmented vegetation into different densities and heights. For a segmentation between ground and vegetation, the metrics planarity, sphericity and normal change rate turned out to be useful. For a segmentation, one of these metrics is sufficient for analyses, and do not need to be combined. In contrast, PCA1 and roughness is less useful. A separation between medium and high vegetation is feasible in a less dense forest. In dense forest, a rough estimation of vegetation boundaries can be implemented with planarity and linearity. In the vertical separation, a clear distinction between meadow and taller vegetation can be taken. Between medium and dense vegetation, deviations can be seen especially in the metrics linearity, volume density and sphericity. In the future, a DEM could be generated based on the metric planarity, preferable in the ULS or MLS data.

The analyses show that path planning is very important for a mobile mapping system in the forest. It dictates how dense the point cloud of objects is and which details are digitised, and which are obscured. This dependency is more apparent on foot within forests than when flying over the canopies. The data acquisition method will strongly influence the point density and intensity. Thus, intensity and volume density is recommended to a limited extent.

More datasets need to be processed to conduct further analysis. Finally, the potential of the metrics result for other tasks should be further tested, for example for machine learning models.

ACKNOWLEDGEMENTS

This study is part of the project “DeepForest: Development of machine learning methods for estimating low forest vegetation from airborne laser point cloud”, funded by the Hessian Ministry of Higher Education, Research, Science, and the Arts’ LOEWE Exploration

program. We thank Marten Krull from 3DVermessung for conducting the ULS flights and providing us with the point clouds.

REFERENCES

Blaser, S.; Meyer, J.; Nebiker, S. (2021): Open urban and forest datasets from a high-performance mobile mapping backpack – a contribution for advancing the creation of digital city twins: The International Archives of the Photogrammetry, Remote Sensing and Spatial Information Sciences (= XLIII-B1-2021), 125–131.

Bundesregierung (2022): So beeinflusst der Klimawandel den Wald. https://www.bundesregierung.de/breg-de/aktuelles/wald-leidet-unter-klimawandel-1661828 (09.11.2022).

Burt, A.; Disney, M.; Calders, K. (2018): Extracting individual trees from lidar point clouds using treeseg. In: Methods in Ecology and Evolution 10(2018)3, 438–445. https://besjournals.onlinelibrary.wiley.com/doi/10.1111/2041-210X.13121.

Chehata, N.; Guo, L.; Mallet, C. (2009): Airborne LiDAR feature selection for urban classification using random forests.

Dassot, M.; Constant, T.; Fournier, M. (2011): The use of terrestrial LiDAR technology in forest science: application fields, benefits and challenges. In: Annals of Forest Science 68(2011)5, 959–974.

Forest DTEP (2023): Forest DTEP – Part of ESA's Digital Twin Earth. About. https://www.foresttwin.org/about (20.07.2023).

Hamraz, H.; Contreras, M.; Zhang, J. (2017): Forest understory trees can be segmented accurately within sufficiently dense airborne laser scanning point clouds. In: Scientific reports 7(2017)1, 6770.

Heinzel, J.; Ginzler, C. (2019): A Single-Tree Processing Framework Using Terrestrial Laser Scanning Data for Detecting Forest Regeneration. In: Remote Sensing 11(2019)1, 60.

Huo, L.; Lindberg, E.; Holmgren, J. (2022): Towards low vegetation identification: A new method for tree crown segmentation from LiDAR data based on a symmetrical structure detection algorithm (SSD). In: Remote Sensing of Environment 270, 112857. https://www.sciencedirect.com/science/article/pii/S0034425721005770.

Iwaszczuk, D.; Koppanyi, Z.; Pfrang, J.; Toth, C. (2019): Evaluation of a mobile multi-sensor system for seamless outdoor and indoor mapping. Warsaw (= Evaluation and Benchmarking Sensors, Systems and Geospatial Data in Photogrammetry and Remote Sensing XLII-1/W2).

Krieg, C. (2020): Merkblatt DWA-M 524. Hydraulische Berechnung von Fließgewässern mit Vegetation. Hennef (= DWA-Regelwerk M 524).

Krisanski, S.; Taskhiri, M.; Gonzalez, Aracil, S.; Herries, D.; Muneri, A.; Gurung, M.; Montgomery, J.; Turner, P. (2021): Forest Structural Complexity Tool – An Open Source, Fully-Automated Tool for Measuring Forest Point Clouds. In: Remote Sensing 13(2021)22, 4677.

Liu, E.; atinfinity (2021): EdwardLiuyc/StaticMapping: Release for DOI.

Meining, S. (2020): Waldzustandsbericht 2020. für den Stadtwald Darmstadt. https://www.darmstadtnews.de/wp-content/uploads/2021/01/Waldzustandsbericht_Darmstadt_2020.pdf.

Nitoslawski, S.; Wong-Stevens, K.; Steenberg, J.; Witherspoon, K.; Nesbitt, L.; van den Konijnendijk Bosch, C. (2021): The Digital Forest: Mapping a Decade of Knowledge on Technological Applications for Forest Ecosystems. In: Earth's Future 9(2021)8.

Russ, T.; Boehnen, C.; Peters, T. (2006): 3D Face Recognition Using 3D Alignment for PCA: 2006 IEEE Computer Society Conference on Computer Vision and Pattern Recognition (CVPR'06) (= 2), 1391–1398.

Song, J.; Zhu, X.; Qi, J.; Pang, Y.; Yang, L.; Yu, L. (2021): A Method for Quantifying Understory Leaf Area Index in a Temperate Forest through Combining Small Footprint Full-Waveform and Point Cloud LiDAR Data. In: Remote Sensing 13(2021)15, 3036.

Vosselman, G.; Maas, H.-G. (2010): Airborne and terrestrial laser scanning. Dunbeath.

Weinmann, M.; Weinmann, M.; Mallet, C.; Brédif, M. (2017): A Classification-Segmentation Framework for the Detection of Individual Trees in Dense MMS Point Cloud Data Acquired in Urban Areas. In: Remote Sensing 9(2017)3, 277.

Wilke, W. (2002): Segmentierung und Approximation großer Punktwolken. (Technische Universität Darmstadt).

Willim, K.; Stiers, M.; Annighöfer, P.; Ammer, C.; Ehbrecht, M.; Kabal, M.; Stillhard, J.; Seidel, D. (2019): Assessing Understory Complexity in Beech-dominated Forests (Fagus sylvatica L.) in Central Europe – From Managed to Primary Forests. In: Sensors (Basel, Switzerland) 19(2019)7.

Xu, W.; Zhang, F. (2020): FAST-LIO: A Fast, Robust LiDAR-inertial Odometry Package by Tightly-Coupled Iterated Kalman Filter.

Zhu, F.; Ren, Y.; Zhang, F. (2022): Robust Real-time LiDAR-inertial Initialization: 2022 IEEE/RSJ International Conference on Intelligent Robots and Systems (IROS), 3948–3955.

AUTHORS

M.Sc. Mona Goebel

TECHNICAL UNIVERSITY OF DARMSTADT
DEPARTMENT OF CIVIL AND ENVIRONMENTAL ENGINEERING SCIENCES – REMOTE SENSING AND IMAGE ANALYSIS

Franziska-Braun-Straße 7 | 64287 Darmstadt | Germany
mona.goebel@tu-darmstadt.de | ORCID: 0000-0002-8291-4791

M.Sc. Jakob Schmidt

TECHNICAL UNIVERSITY OF DARMSTADT
DEPARTMENT OF CIVIL AND ENVIRONMENTAL ENGINEERING SCIENCES – MEASURING SYSTEMS AND SENSOR TECHNOLOGY

Franziska-Braun-Straße 7 | 64287 Darmstadt | Germany
jakob.schmidt1@tu-darmstadt.de | ORCID: 0000-0002-1733-1258

Prof. Dr.-Ing. Dorota Iwaszczuk

TECHNICAL UNIVERSITY OF DARMSTADT
DEPARTMENT OF CIVIL AND ENVIRONMENTAL ENGINEERING SCIENCES – REMOTE SENSING AND IMAGE ANALYSIS

Franziska-Braun-Straße 7 | 64287 Darmstadt | Germany
dorota.iwaszczuk@tu-darmstadt.de | ORCID: 0000-0002-5969-8533

Manuskript eingereicht: 26.04.2023 | Im Peer-Review-Verfahren begutachtet